



# Mass transfer from single carbon-dioxide bubbles in electrolyte aqueous solutions in vertical pipes



Yohei Hori, Kosuke Hayashi, Shigeo Hosokawa, Akio Tomiyama\*

Graduate School of Engineering, Kobe University, 1-1 Rokkodai, Nada, Kobe, Hyogo 657-8501, Japan

## ARTICLE INFO

### Article history:

Received 14 March 2017

Received in revised form 14 June 2017

Accepted 19 July 2017

### Keywords:

Sodium chloride (NaCl)

Sherwood number

Taylor bubble

Diffusion coefficient

## ABSTRACT

Mass transfer rates,  $k_L$ , of single carbon-dioxide ( $\text{CO}_2$ ) bubbles rising through vertical pipes filled with electrolyte aqueous solutions were measured to investigate the effects of the presence of electrolyte on  $k_L$ . Sodium chloride (NaCl) was used for electrolyte and its concentration was varied from 3.5 to 14 wt.%. The pipe diameters,  $D$ , were 12.5, 18.2 and 25.0 mm and the bubble diameter,  $d$ , ranged from 5 to 25 mm. The diameter ratio,  $\lambda (= d/D)$ , was varied from 0.2 to 1.7, to cover various bubble shapes, i.e. ellipsoidal, cap, semi-Taylor bubbles and Taylor bubbles. The conclusions obtained are as follows: (1)  $k_L$  in the NaCl aqueous solutions decreases with increasing the NaCl concentration mainly due to the reduction of the diffusion coefficient of  $\text{CO}_2$  in the liquid phase, (2) the Sherwood numbers,  $Sh$ , of Taylor bubbles of  $L/D > 1$  in the NaCl aqueous solutions can be well evaluated using the available Sherwood number correlation for clean Taylor bubbles, where  $L$  is the length of a Taylor bubble, (3)  $Sh$  of ellipsoidal, cap, semi-Taylor bubbles and Taylor bubbles of  $L/D \leq 1$  in the clean water and NaCl aqueous solutions can be well correlated in terms of the Peclet number and the dimensionless bubble diameter  $d^* = d/d_T$ , where  $d_T$  is the bubble diameter at the transition from the ellipsoidal-cap bubble regime to the semi-Taylor bubble regime, and (4) the  $Sh$  correlations give good predictions for long-term bubble dissolution processes in NaCl aqueous solutions.

© 2017 Elsevier Ltd. All rights reserved.

## 1. Introduction

Mass transfer between bubbles and liquid has been utilized in many industrial applications such as chemical reactors [1], bioreactors and sequestration of carbon dioxide ( $\text{CO}_2$ ) in ocean [2]. The mass transfer rate,  $k_L$ , is known to depend on various factors such as the diameter, shape and rise velocity of a bubble, the physical properties of the two phases and the presence of a pipe wall and impurities, e.g. surface-active agents (surfactants) and surface-inactive electrolytes. A number of studies have, therefore, been carried out to investigate the effects of these factors on  $k_L$  and many  $k_L$  correlations have been proposed [3].

Hosoda et al. [4] investigated the effects of the wall of a vertical pipe on mass transfer from single clean bubbles of various shapes such as ellipsoidal and Taylor bubbles. They proposed a  $k_L$  correlation by taking into account the wall effect on  $k_L$  of clean bubbles. The  $k_L$  of fully-contaminated bubbles under the wall effect was reported by Aoki et al. [5–7]. The adsorption of surfactant reduces the surface tension and a resulting non-uniform distribution of

surface tension causes a force tangential to the interface, i.e. the Marangoni force, by which shape oscillation and capillary waves at the interface are attenuated and the rise velocity and  $k_L$  of ellipsoidal bubbles are significantly decreased. Numerical simulations of Taylor bubbles contaminated with Triton X-100 [6] showed that the surfactant effect on the bubble velocity and  $k_L$  is small since Triton X-100 is apt to accumulate only in the bubble tail region. On the other hand, alcohols affect the rise velocity and  $k_L$  of a Taylor bubble since they cover the whole interface [7]. Aoki et al. proposed  $k_L$  correlations applicable to ellipsoidal and Taylor bubbles fully-contaminated with Triton X-100 [6] and with alcohols of various carbon-chain lengths [7] by taking into account the above-mentioned surfactant effects on  $k_L$ .

The presence of electrolyte also affects the surface tension, i.e., the surface tension increases with increasing the electrolyte concentration [8]. The electrolyte is also known to reduce the diffusion coefficients of gaseous species in liquid [9] and the solubility of the gas phase [10]. However there are few studies on the effects of the electrolyte on  $k_L$  of bubbles. Baz-Rodriguez et al. [11] and Ruenngam et al. [12] carried out experiments on mass transfer in bubbly flows in bubble columns and reported that the presence of electrolyte decreases the net mass transfer rate in the bubbly flows. To understand the cause of this decrease, the effects of the

\* Corresponding author at: Department of Mechanical Engineering, Graduate School of Engineering, Kobe University, Japan.

E-mail address: [tomiyama@mech.kobe-u.ac.jp](mailto:tomiyama@mech.kobe-u.ac.jp) (A. Tomiyama).

electrolyte on  $k_L$  of single bubbles should be investigated. In addition, the effects of the electrolyte on  $k_L$  of bubbles under the influence of the presence of walls, which largely affect the bubble shape and velocity, have not been investigated, and our knowledge on them is still insufficient.

The  $k_L$  of single CO<sub>2</sub> bubbles rising through electrolyte aqueous solutions in vertical pipes were measured in this study to investigate the effects of the electrolyte on  $k_L$ . Sodium chloride (NaCl) aqueous solutions were used for the liquid phase. The pipe diameters,  $D$ , were 12.5, 18.2 and 25.0 mm. The diameter ratio,  $\lambda$ , which is the ratio of the sphere-volume-equivalent bubble diameter,  $d$ , to  $D$ , was widely varied to cover various bubble shapes such as ellipsoidal, cap, semi-Taylor and Taylor bubbles. The applicability of  $k_L$  correlations to long-term bubble dissolution processes in the NaCl aqueous solutions was examined through comparisons with the data.

## 2. Experimental

Fig. 1 shows the experimental setup, which consists of the vertical pipe, the lower and upper tanks and the reservoir. The upper tank and the reservoir were open to the atmosphere, and therefore, the gas components in the liquid were in their equilibrium to the atmosphere. Three pipes of  $D = 12.5, 18.2$  and  $25.0$  mm were used. The pipe length was 2000 mm. The reference elevation ( $z = 0$  mm) was set at 1900 mm below the water surface in the upper tank. The pipe was made of fluorinated-ethylene-propylene (FEP) resin. The FEP pipe was installed in the acrylic duct. Water was filled in the gap between the duct and the pipe to reduce optical distortion in bubble images. Water purified using a Millipore system (Elix 3) and CO<sub>2</sub> of 99.9 vol.% purity were used for the liquid and gas phases, respectively. NaCl was used for the electrolyte. The concentrations,  $C$ , of NaCl were 3.5, 7.0 and 14 wt.%. The physical properties of the liquid and gas phases are shown in Table 1, where  $\rho_L$  is the liquid density,  $\mu_L$  the liquid viscosity,  $\sigma$  the surface tension,  $D_L$

the diffusion coefficient of CO<sub>2</sub> in the liquid phase [9], and  $C_s$  the CO<sub>2</sub> concentration at bubble surface [10]. The increase in  $C$  increases  $\sigma$  due to the surface-inactive nature of NaCl, whereas  $D_L$  and  $C_s$  decrease with increasing  $C$ .

Experiments were carried out at atmospheric pressure and room temperature ( $298 \pm 1.0$  K). The liquid in the pipe was refreshed before each run by circulating the liquid using a pump. A predetermined amount of CO<sub>2</sub> gas was injected from the bottom of the lower tank and stored in the hemispherical cup by using the gastight syringe. A single bubble was released by rotating the cup. Front and side images of a bubble in the test section were recorded using the two synchronized video cameras (Integrated Design Tool, M3, frame rate: 250 frame/s, exposure time: 1000  $\mu$ s, spatial resolution: 0.04–0.05 mm/pixel), which were mounted on the  $z$ -axis actuators (SUS Corp., SA-S6AM). The green and red LED light sources (NICHIA, NSPG510AS; ROHM, SLI-580UT3F) were used for back illumination. The motion of the cameras and the LED lights were synchronized using the actuators. Bubbles were tracked for  $0 \leq z \leq 550$  mm.

An image processing method [4] was utilized to measure bubble volumes, diameters and positions. The original gray-scale images were transformed into binary images. By assuming that the horizontal cross sections of a bubble were elliptical, a three-dimensional bubble shape was reconstructed by piling up the elliptic disks. The bubble diameter,  $d$ , was evaluated from the volume of the reconstructed bubble shape. The rise velocities,  $V_B$ , of bubbles in the stagnant liquids were calculated from the rates of change in the axial bubble position. Uncertainties estimated at 95% confidence in  $d$  and  $V_B$  were  $\pm 2.1\%$  and  $0.20\%$ , respectively. The  $d$  ranged from 5 to 25 mm, and therefore, the ranges of  $\lambda$  were 0.4–1.7, 0.3–1.4 and 0.2–1.0 for  $D = 12.5, 18.2$  and  $25.0$  mm, respectively.

The  $k_L$  and the Sherwood number,  $Sh$ , were evaluated from the rate of decrease in  $d$ . When a flow is isothermal, the change in the moles,  $n$ , of CO<sub>2</sub> inside a bubble is given by

$$\frac{dn}{dt} = -k_L A (C_s - C_0) \quad (1)$$

where  $t$  is the time,  $A (= \pi d^2)$  the bubble surface area, and  $C_0$  the CO<sub>2</sub> concentration in the liquid phase. By assuming that  $C_s$  is given by Henry's law, the mole fraction of CO<sub>2</sub> in a bubble is close to unity and  $C_0 \ll C_s$ , Eq. (1) can be rewritten as

$$k_L = -\frac{1}{\pi d^2} \frac{H - P(z)X}{C_L P(z)X} \frac{dn}{dt} \quad (2)$$

where  $H$  is the Henry constant,  $X$  the mole fraction of CO<sub>2</sub>,  $C_L$  the H<sub>2</sub>O concentration (55.4 kmol/m<sup>3</sup>), and  $P$  the pressure inside a bubble given by

$$P(z) = P_{atm} + \rho_L g h(z) \quad (3)$$

where  $P_{atm}$  is the atmospheric pressure,  $g$  the acceleration of gravity, and  $h(z)$  the distance from the free surface to the bubble center. The mole fraction  $X$  in Eq. (2) was assumed to be unity, since the bubble arrived at the test section within 10 s after the injection of CO<sub>2</sub> gas into the hemispherical cup so that the change in the gas composition inside a bubble was negligible. By assuming that CO<sub>2</sub> is an ideal gas,  $dn/dt$  can be expressed in terms of  $P$  and  $d$  as follows:

$$\frac{dn}{dt} = \frac{\pi}{6RT} \frac{d(Pd^3)}{dt} \quad (4)$$

where  $R$  is the universal gas constant. The  $k_L$  was calculated by substituting Eq. (4) into Eq. (2) and evaluating  $d(Pd^3)/dt$  by using the centered difference between  $t_1$  and  $t_2$ :

$$k_L = \frac{(H - P_{12})(P_2 d_2^3 - P_1 d_1^3)}{6RT(t_2 - t_1) d_{12}^3 C_L P_{12}} \quad (5)$$

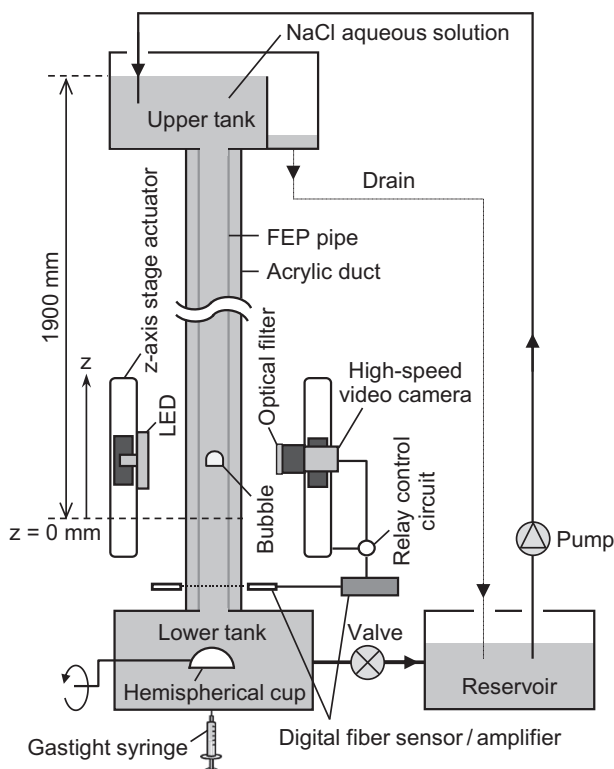


Fig. 1. Experimental setup.

Download English Version:

<https://daneshyari.com/en/article/4993499>

Download Persian Version:

<https://daneshyari.com/article/4993499>

[Daneshyari.com](https://daneshyari.com)